Letter

Non-Hermitian $C_{\mathrm{NH}} = 2$ Chern insulator protected by generalized rotational symmetry

Kai Chen* and Alexander B. Khanikaev†

Department of Physics, City College of New York, New York, New York 10031, USA;
Department of Electrical Engineering, Grove School of Engineering, City College of the City University of New York, 140th Street and Convent Avenue, New York, New York 10031, USA;
and Physics Program, Graduate Center of the City University of New York, New York, New York 10016, USA

(Received 28 November 2021; revised 27 January 2022; accepted 11 February 2022; published 24 February 2022)

We propose a non-Hermitian topological system protected by the generalized rotational symmetry which invokes rotation in space and Hermitian conjugation. The system, described by the tight-binding model with reciprocal imaginary next-nearest-neighbor hopping, is found to host two pairs of in-gap edge modes in the gapped topological phase, and is characterized by the non-Hermitian (NH) Chern number $C_{\mathrm{NH}} = 2$. The quantization of the NH Chern number is shown to be protected by the generalized rotational symmetry $\hat{H}^{+}(g\vec{k}) = \hat{U}_g \hat{H}(\vec{k}) \hat{U}_g^{+}$ of the system. Our finding paves the way towards non-Hermitian topological systems characterized by large values of topological invariants and hosting multiple in-gap edge states, which can be used for topologically resilient multiplexing.

DOI: 10.1103/PhysRevB.105.L081112

I. INTRODUCTION

Topological phases represent a new state of matter which extends beyond the conventional symmetry-based Landau paradigm [1,2]. The first, and perhaps the most recognized, topological phase in modern physics is the integer quantum Hall insulator (IQHI) [3,4]. IQHI is characterized by an integer number of edge states at the interface between the quantum Hall insulator and a trivial insulator, with the number of edge states and the quantized edge conductance determined by the Chern number, the topological invariant which is totally defined by the bulk band topology of the system [5]. Since the discovery of the IQHI, the topological concepts started to play an increasingly important role in our understanding and classification of materials [6,7], blossoming into a new research field of condensed-matter physics, and even spilling into classical domains of topological acoustics, mechanics, and photonics [8–11].

The celebrated Altland-Zirnbauer (AZ) "tenfold way" [12] allows to discern any topological quantum system by its pattern of nonspatial symmetries, i.e., chiral symmetry, particle-hole symmetry, and time-reversal symmetry. Taking into consideration spatial symmetries allowed introducing the concept of topological crystalline phases [13] characterized by gapped ground states that are not adiabatically connected to an atomic limit as long as certain spatial symmetries, which include mirror and rotational symmetries, are preserved. While originally limited to purely Hermitian systems, in the recent years, the non-Hermitian models has brought new flavors to topological physics [14–23]. The non-Hermitian systems were found to host novel phenomena, including without direct Hermitian analogs. One example is the generalized bulk-edge correspondence [24–28], which represents a guiding principle of Hermitian topological matter, and can break down in the non-Hermitian settings. For instance, a system with open boundary conditions cannot be understood by studying the band topology of the system with periodic boundary condition [29]. Other examples include new class of "skin" boundary states [30–32] and non-Hermitian exceptional points [33–35] unique to non-Hermitian systems, and even totally new topological phases enabled by the additional imaginary dimension of the energy spectrum [36,37]. The tenfold AZ symmetry classification in Hermitian systems has been recently extended to a 38-fold classification in non-Hermitian systems to encompass the distinction between complex conjugation and transposition for non-Hermitian Hamiltonian [23]. We note, however, that the generalized rotational symmetry proposed here, $\hat{H}^{+}(g\vec{k}) = \hat{U}_g \hat{H}(\vec{k}) \hat{U}_g^{+}$, does not belong to this extended 38-fold symmetry classification. This is due to the fact that the respective 38-fold symmetry classification only considers nonspatial symmetries. Introduction of additional spatial symmetries would require a further expansion of the topological classification [22], a direction worth of a separate rigorous study.

While some non-Hermitian generalizations of the IQHI have been reported in literature [38,39], the systems considered so far were characterized by a non-Hermitian (NH) Chern number $C_{\mathrm{NH}} = \pm 1$ and thus could only allow existence of a single edge state (or a pair of edge states for the case of domain-wall geometry) in the topologically nontrivial gap. On the other hand, higher values of topological invariants can be of interest and may also be highly desirable for numerous practical applications due to the possibility of multiplexing via several boundary modes [40]. Thus, it is worth exploring the physics and the possibility of a non-Hermitian Chern insulator with higher non-Hermitian Chern number

*kchen3@gradcenter.cuny.edu
†akhanikaev@ccny.cuny.edu

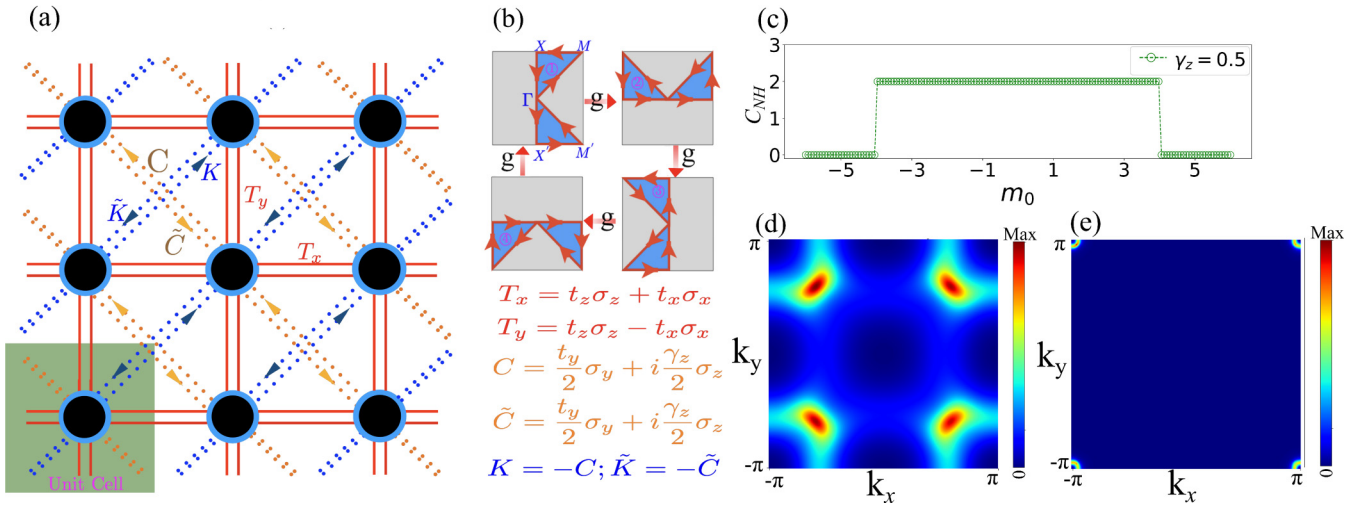

FIG. 1. (a) Schematic of the proposed non-Hermitian tight-binding model. (b) The first BZ and high-symmetric points of the model. (c) The non-Hermitian Chern number $C_{\rm NH}$ as a function of parameter m_0 with $\gamma_z = 0.5$, and $t_x = t_y = t_z = 1$. (d), (e) Imaginary part of the Berry curvature distribution over the first BZ for the occupied band for (d) $m_0 = 1$ and (e) $m_0 = 3.95$, close to topological transition.

$|C_{\rm NH}| \geqslant 2$, which, to the best of our knowledge, have not yet been discovered.

In this work, we build upon prior work on Hermitian model [41] characterized by higher Chern number values, and we propose a non-Hermitian system with higher non-Hermitian topological invariant, the Chern number $C_{\rm NH} = 2$. The system is described by a non-Hermitian tight-binding model which is shown to host two unidirectional edge states at a single boundary within a topological gap. We prove that the reported topological phase and the edge states are protected by a generalized rotational symmetry which invokes both spatial rotation and Hermitian conjugation. Specifically, we find that the generalized rotation symmetry for our proposed non-Hermitian Hamiltonian ensures quantization of the non-Hermitian Chern number, which, in turn, defines the net number of edge modes, thus establishing a generalized non-Hermitian bulk boundary correspondence. Similar to the case of Hermitian Chern insulators, the non-Hermitian Chern number does not allow predicting the boundary behavior of the finite-size model for the case of gapless bulk bands, because the Berry connection is not well defined.

II. THE TIGHT-BINDING MODEL AND AN ELEVATED NON-HERMITIAN CHERN NUMBER

In what follows, we consider a non-Hermitian tight-binding model with complex next-nearest-neighbor (NNN) coupling as depicted in Fig. 1(a). This model is found to exhibit two distinct gapped phases, topological and trivial gapped phases, which are separated by the gapless phase. The topological gapped phase hosts two pairs of in-gap edge modes. As detailed below, the topological phase and the edge states are protected by the generalized rotational symmetry for the non-Hermitian Hamiltonian $\hat{U}_g\ \hat{H}(\vec{gk})\hat{U}_g^{+} = \hat{H}^{+}(\vec{k})$, where $\hat{U}_g$ is the unitary representation of the generator $g \equiv R_z(\frac{\pi}{2})$ of the fourfold rotational group C_4. In our model it is the unitary matrix $\hat{U}_g \equiv e^{-(i\pi/2)\hat{\sigma}_z}$.

The generalized rotational symmetry quantizes the non-Hermitian Chern number (see Supplemental Material for details [42]), which assumes value $C_{\rm NH} = 2$ in topological gapped phase, which explains the emergence of a pairs of in-gap edge states at each boundary of the system. The non-Hermitian Chern number used here represents a direct analog of the Hermitian Chern number and can be expressed in the form $C_{\rm NH} \equiv \frac{1}{2\pi i}\iint_{BZ}\vec{B}_n(\vec{k})\,dk^2$, where $\vec{B}_n(\vec{k}) = \nabla_{\vec{k}} \times \vec{A}_n(\vec{k})$ is the non-Hermitian Berry curvature. The difference with the Hermitian version lies in the fact that the non-Hermitian Berry connection should be evaluated with the use of the left and right eigenstates of the non-Hermitian Hamiltonian, i.e., $\vec{A}_n(\vec{k}) \equiv \langle\phi_n(\vec{k})|\nabla_{\vec{k}}\,|\psi_n(\vec{k})\rangle$, where the vector $\langle\phi_n(\vec{k})|$ ($|\psi_n(\vec{k})\rangle$) is the left (right) eigenstate of the non-Hermitian Hamiltonian $\hat{H}(\vec{k})$, i.e., $\langle\phi_n(\vec{k})|\ \hat{H}(\vec{k}) = \epsilon_n(\vec{k})\langle\phi_n(\vec{k})|$ and $\hat{H}(\vec{k})|\psi_n(\vec{k})\rangle = \epsilon_n(\vec{k})|\psi_n(\vec{k})\rangle$, and where n is the band index. We would like to emphasize one important property of the non-Hermitian matrix, that its left (right) eigenstates corresponding to different eigenvalues may not be orthogonal with each other; however, the left eigenstate with eigenvalue ϵ_1 and the right eigenstate with eigenvalue ϵ_2 are orthogonal as long as $\epsilon_1 \neq \epsilon_2$.

The tight-binding Hamiltonian of the proposed system [Fig. 1(a)] in real space is defined as

$$\hat{H} = m_0\sum_{m,n}(a^{+}_{m,n}a_{m,n} - b^{+}_{m,n}\,b_{m,n}) + t_x\sum_{m,n}[(a^{+}_{m,n}b_{m+1,n} + a^{+}_{m+1,n}b_{m,n} - a^{+}_{m,n}b_{m,n+1} - a^{+}_{m,n+1}b_{m,n}) + \text{H.c.}]$$

$$+ t_y\sum_{m,n}\left[\frac{i}{2}(b^{+}_{m,n}a_{m+1,n-1} + b^{+}_{m,n}a_{m-1,n+1} - b^{+}_{m,n}a_{m+1,n+1} - b^{+}_{m,n}a_{m-1,n-1}) + \text{H.c.}\right]$$

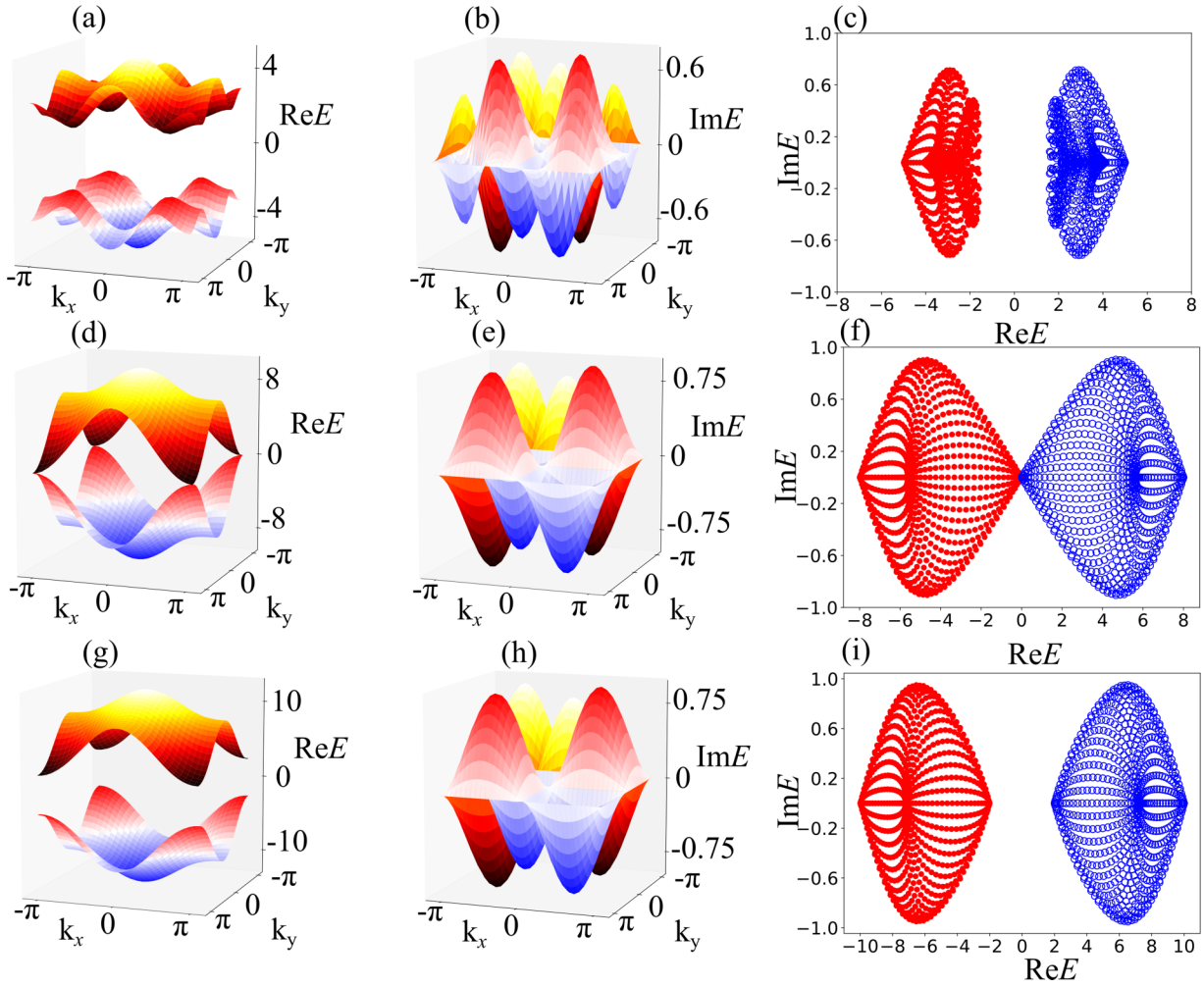

FIG. 2. (a), (b) Real and imaginary parts of the bulk energy spectra for $m_0 = 1$ (topological phase), and (c) respective complex energy spectra of two bulk bands (red and blue regions) in the complex energy plane for $m_0 = 1$. (d), (e) Real and imaginary parts of the bulk energy spectra for $m_0 = 4$ (gapless phase) and (f) respective complex energy spectra of two bulk bands for $m_0 = 4$. (g), (h) Real and imaginary parts of bulk energy spectra for $m_0 = 6$ (trivial phase), and (i) respective complex energy spectra of two bulk bands for $m_0 = 6$.

$$
\begin{aligned}
&+ t_z \sum_{m,n} [(a^+_{m,n} a_{m+1,n} + a^+_{m,n} a_{m,n+1} - b^+_{m,n} b_{m+1,n} - b^+_{m,n} b_{m,n+1}) + \text{H.c.}] \\
&- \frac{i\gamma_z}{2} \sum_{m,n} (a^+_{m,n} a_{m+1,n+1} + a^+_{m,n} a_{m-1,n-1} - a^+_{m,n} a_{m+1,n-1} - a^+_{m,n} a_{m-1,n+1} \\
&+ b^+_{m,n} b_{m+1,n-1} + b^+_{m,n} b_{m-1,n+1} - b^+_{m,n} b_{m+1,n+1} - b^+_{m,n} b_{m-1,n-1}). \qquad (1)
\end{aligned}
$$

In the tight-binding model described by Eq. (1) we assumed that there are two degrees of freedom (represented by states A and B) at each site, with $a_{m,n}$ ($b_{m,n}$) and $a^+_{m,n}$ ($b^+_{m,n}$) representing annihilation and creation operators for the state A (B). States A and B can be of different energy m_0 and $-m_0$, and t_x is the nearest-neighbor (NN) hopping amplitude between the states A (states B) of the neighboring unit cells, t_y is the NNN hopping amplitude between state A and state B, t_z is the NN hopping amplitude between state A (B) and itself. The $-i\,\gamma_z$ ($i\,\gamma_z$) represent complex NNN hopping between A states (and B states), which introduces non-Hermicity into our tight-binding model. In this paper, we set $t_x = t_y = t_z = 1$ without loss of generality. The Hamiltonian equation (1) can be expressed in the momentum space as

$$
\begin{aligned}
\hat{H}(k_x, k_y) = {} & 2t_x(\cos k_x - \cos k_y)\hat{\sigma}_x + t_y[\cos(k_x - k_y) \\
& - \cos(k_x + k_y)]\hat{\sigma}_y \\
& + [m_0 + 2t_z(\cos k_x + \cos k_y) \\
& + i2\gamma_z \sin k_x \sin k_y)]\hat{\sigma}_z, \qquad (2)
\end{aligned}
$$

where $\{\hat{\sigma}_x, \hat{\sigma}_y, \hat{\sigma}_z\}$ are Pauli matrices acting in the Hilbert space spanned by the states A and B, and the momentum $\vec{k} = (k_x, k_y)$ is mapped to $(gk_x, gk_y) \equiv R_z(\frac{\pi}{2})(k_x, k_y) =$

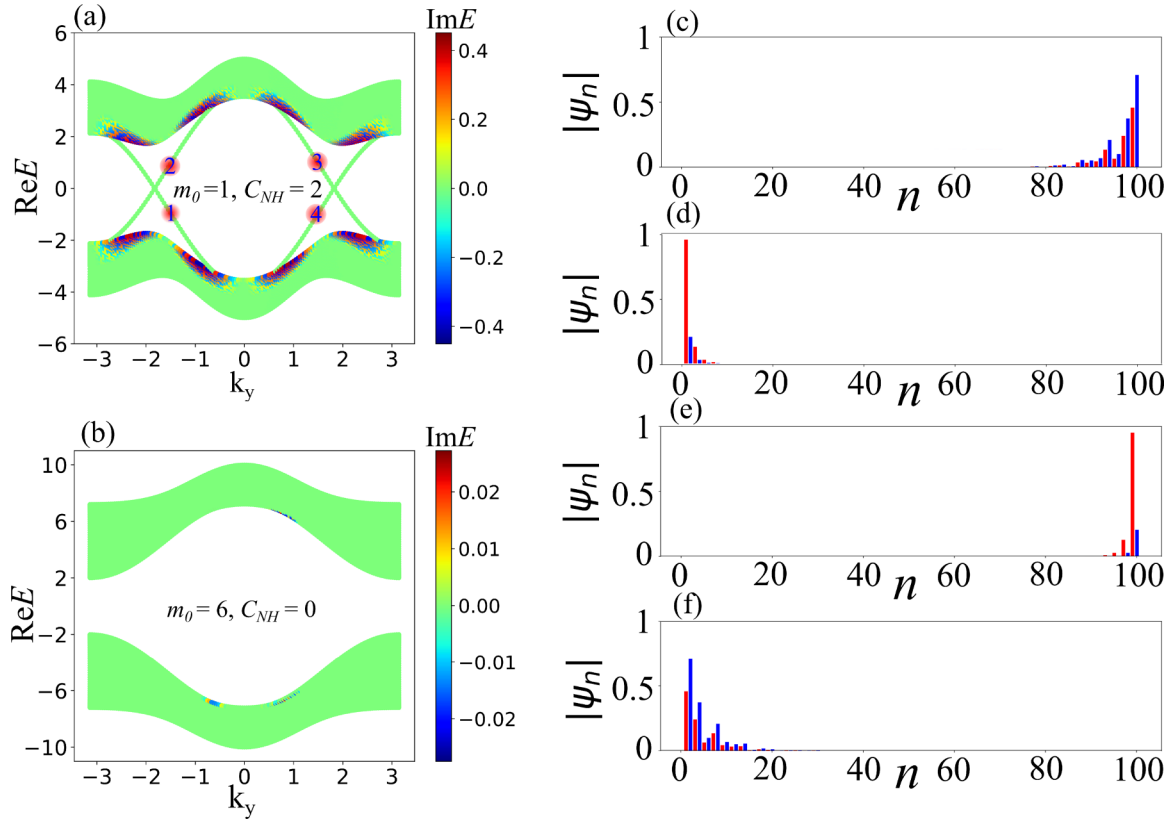

FIG. 3. (a), (b) The complex energy spectrum for different values of m_0 for the supercell with periodic boundary conditions in the y direction. (c)–(f) The wave-function amplitude of the edge states indicated by the numbers 1 to 4 in (a). The number of sites along x direction is $n_x = 50$, the amplitude of the wave function at state A (B) shown by the red (blue) histogram.

$(k_y, -k_x)$ under counterclockwise $\frac{\pi}{2}$ rotation around the z axis. It is not hard to see for the Hamiltonian in the momentum space that it possesses the generalized rotational symmetry defined as $\hat{H}^+(gk_x, gk_y) = \hat{U}_g \hat{H}(k_x, k_y)\hat{U}_g^+$ with $\hat{U}_g = e^{-(i\pi/2)\hat{\sigma}_z}$, and one can also show that the Hamiltonian with opposite momentum $\vec{k}$ can be obtained by applying the operator twice, e.g., $\hat{U}_g^2$.

We would like to emphasize that the systems described by the Hamiltonian equations (1) and (2) can be brought to gapless phase by properly tuning the parameters γ_z and m_0; however, in this work, we are interested in the gapped phase of non-Hermitian Chern insulator with higher non-Hermitian Chern number and multiple edge modes, and the case of the Chern number $C_{\rm NH} = 2$ specifically. Therefore, we focus on the values of parameters that ensure the existence of a line gap in the complex energy plane.

In our model, due to the form of the symmetry operator $\hat{U}_g$, the non-Hermitian Chern number can be calculated by evaluating the expectation value of $\hat{\sigma}_z$ with respect to the right eigenstates at the high-symmetry points in the first Brillouin zone:

$$C_{\rm NH} = \frac{2}{\pi} \,\mathrm{Im} \oint_\gamma \vec{A}_n(\vec{k}) d\vec{k} = \frac{2}{\pi} \left[2\theta_g(X) - 3\theta_g(\Gamma) + \theta_g(M)\right] (\mathrm{mod}\ 4), \quad (3)$$

where γ represent the loop in the first Brillouin zone, as shown in Fig. 1(b), $\theta_g(\vec{K}) = \frac{\pi}{2}\langle\psi_n(g\vec{K})|\hat{\sigma}_z|\psi_n(\vec{K})\rangle$, $\vec{K} \in \{\Gamma,\ X,\ M\}$, and $|\psi_n(\vec{K})\rangle$ is the right eigenstate corresponding to eigenvalue with the negative real part.

We first calculate the non-Hermitian Chern number as function of m_0 with $\gamma_z = 0.5$. As shown in Fig. 1(c), for $m_0 \in (-4,\ 4)$, the system is in the topological gapped phase with the non-Hermitian Chern number $C_{\rm NH} = 2$, and for other values of m_0, the non-Hermitian Chern number vanishes, $C_{\rm NH} = 0$, bringing the system to the trivial phase. At $m_0 = \pm 4$, the gap closes and the system transitions from the topological gapped phase to the trivial gapped phase, as shown in Fig. 2.

The generalized rotation symmetry of our non-Hermitian model restricts the Berry connection in the first Brillouin zone (BZ) to satisfy the following equation:

$$\vec{A}_n(g^l\vec{k}) = \begin{cases} g^l[\vec{A}_n(\vec{k}) + i\, l\, \nabla_{\vec{k}}\, \theta_g(\vec{k})] & \text{for } l \in 2Z \\ g^l[-\vec{A}_n^*(\vec{k}) + i\, l\, \nabla_{\vec{k}}\, \theta_g(\vec{k})] & \text{for } l \in 2Z+1 \end{cases}. \quad (4)$$

For a non-Hermitian system, the respective non-Hermitian Berry curvature $\vec{B}_n(\vec{k}) = \nabla_{\vec{k}} \times \vec{A}_n(\vec{k})$ assumes complex values in general; therefore, the non-Hermitian Chern number $C_n \equiv \frac{1}{2\pi i}\iint_{BZ} \vec{B}_n(\vec{k})\, d\vec{k}^2$ is complex. However, according to Eq. (4), the real part of the non-Hermitian Berry curvature

at $\vec{k}$ cancels with the real part of the non-Hermitian Berry curvature at $R_z(\frac{\pi}{2})\vec{k}$, leading to the net zero value of the imaginary part of the non-Hermitian Chern number.

Inspection of the imaginary part of the non-Hermitian Berry curvature in the BZ for the topological gapped phase reveals four peaks, shown in Figs. 1(d) and 1(e), with each peak contributing 1/2 to the real part of the non-Hermitian Chern number. At the same time, Eq. (4) ensures that there exist four equivalent peaks in the imaginary part of the non-Hermitian Berry curvature, as shown in Figs. 1(d) and 1(e), thus yielding total non-Hermitian Chern number of 2 in the topological gapped phase. Figures 1(d) and 1(e) reveal how the position of the imaginary part of the non-Hermitian Berry curvature changes with the parameter m_0, indicating that there always exist four equivalent peaks in the first Brillouin zone for the topological gapped phase. This evolution clearly shows that the higher value of the Chern number originates from the four corners of the Brillouin zone, which are not equivalent due to the non-Hermitian character of the system, thus allowing these corners to manifest as four effective valleys (regions in the momentum space) each contributing equal value of 1/2 to the net non-Hermitian Chern number.

The Chern number in the Hermitian IQHI predicts number of unidirectional boundary states supported at an interface—-the principle known as the bulk-boundary correspondence [43,44]. Similarly, the non-Hermitian Chern number is related to the net number of unidirectional edge states localized at the interface between topological and trivial system. To confirm the bulk-edge correspondence in our non-Hermitian model, we study a system with periodic boundary condition in the y direction and open boundary condition in the x direction, thus forming a cylindrical (supercell) geometry. The energy spectrum for this geometry (as function of k_y) is shown in Figs. 3(a) and 3(b). For $m_0 = 1$, the system is in the topologically nontrivial phase with $C_{NH} = 2$, and there exist two pairs of edge states in the gap which, as shown in Figs. 3(c)–3(f), are both localized to the edges of the cylinder. The spectrum of these states is a purely real number, which implies that the edge modes of our non-Hermitian model are dissipationless. Inspection of the wave functions of the edge states reveals that for the states shown in Figs. 3(c) and 3(f) the phase difference between A and B components at each site is zero (A and B are in phase), while for the edge states in Figs. 3(d) and 3(e) the phase difference is π (A and B are out of phase). As expected, no edge states are found in Fig. 3(b) corresponding to the topologically trivial phase, when non-Hermitian Chern number $C_{NH} = 0$. The band structure and edge states for cylinder geometry with periodic boundary in the x direction and open boundary condition in the y direction are similar (see Supplemental Material, Sec. II [42]). In the Supplemental Material [42], we also calculate the non-Hermitian Chern number based on the open-bulk Chern number [45] with open boundaries in both x and y directions. The open-bulk Chern number's predictions agree with the predictions calculated by our non-Hermitian Chern number, Eq. (3). These observations confirm the bulk-edge correspondence of our non-Hermitian model.

III. CONCLUSIONS

In this work, we proposed a two-band model of a non-Hermitian topological insulator supporting a higher-valued non-Hermitian Chern number $C_{NH} = 2$, which, as the result, hosts two edge states with purely real spectrum in the topologically nontrivial band gap. More importantly, we develop a mathematical formalism and prove that the quantization of the non-Hermitian Chern number is protected by the generalized C_4 rotational symmetry present in our system and invoking the $\frac{\pi}{2}$ rotation along with the Hermitian conjugation operation (exchange of gain and loss). Our work shows the possibility to generalize the rotational symmetry, commonly used to describe Hermitian systems, and employ non-Hermitian character of systems to induce higher values of the topological invariants, such as the non-Hermitian Chern number. Our work thus outlines an approach to engineer physical systems supporting elevated number of edge states at the boundaries of non-Hermitian topological systems by judicious introduction of gain and loss, which may enable applications with robust guiding and multiplexing over multiple boundary states.

ACKNOWLEDGMENTS

The work was supported by the NSF Grants No. DMR-1809915 and No. OMA-1936351, the ONR Award No. N00014-21-1-2092, and the Simons Collaboration on Extreme Wave Phenomena.

[1] M. Z. Hasan and C. L. Kane, Rev. Mod. Phys. **82**, 3045 (2010).
[2] X.-L. Qi and S.-C. Zhang, Rev. Mod. Phys. **83**, 1057 (2011).
[3] K. v. Klitzing, G. Dorda, and M. Pepper, Phys. Rev. Lett. **45**, 494 (1980).
[4] K. Von Klitzing, Rev. Mod. Phys. **58**, 519 (1986).
[5] D. J. Thouless, M. Kohmoto, M. P. Nightingale, and M. den Nijs, Phys. Rev. Lett. **49**, 405 (1982).
[6] A. P. Schnyder, S. Ryu, A. Furusaki, and A. W. Ludwig, Phys. Rev. B **78**, 195125 (2008).
[7] C.-K. Chiu, J. C. Teo, A. P. Schnyder, and S. Ryu, Rev. Mod. Phys. **88**, 035005 (2016).
[8] T. Ozawa, H. M. Price, A. Amo, N. Goldman, M. Hafezi, L. Lu, M. C. Rechtsman, D. Schuster, J. Simon, O. Zilberberg, and I. Carusotto, Rev. Mod. Phys. **91**, 015006 (2019).
[9] L. Lu, J. D. Joannopoulos, and M. Soljačić, Nat. Photonics **8**, 821 (2014).
[10] A. B. Khanikaev and G. Shvets, Nat. Photonics **11**, 763 (2017).
[11] G. Ma, M. Xiao, and C. T. Chan, Nat. Rev. Phys. **1**, 281 (2019).
[12] A. Altland and M. R. Zirnbauer, Phys. Rev. B **55**, 1142 (1997).
[13] L. Fu, Phys. Rev. Lett. **106**, 106802 (2011).
[14] C. M. Bender and S. Boettcher, Phys. Rev. Lett. **80**, 5243 (1998).
[15] Z. Gong, Y. Ashida, K. Kawabata, K. Takasan, S. Higashikawa, and M. Ueda, Phys. Rev. X **8**, 031079 (2018).
[16] Y. Ashida, Z. Gong, and M. Ueda, Adv. Phys. **69**, 249 (2020).
[17] L. Feng, R. El-Ganainy, and L. Ge, Nat. Photonics **11**, 752 (2017).

[18] K. Y. Bliokh, D. Leykam, M. Lein, and F. Nori, Nat. Commun. **10**, 1 (2019).
[19] X. Ni, D. Smirnova, A. Poddubny, D. Leykam, Y. Chong, and A. B. Khanikaev, Phys. Rev. B **98**, 165129 (2018).
[20] M. Li, X. Ni, M. Weiner, A. Alù, and A. B. Khanikaev, Phys. Rev. B **100**, 045423 (2019).
[21] C. C. Wojcik, X.-Q. Sun, T. Bzdušek, and S. Fan, Phys. Rev. B **101**, 205417 (2020).
[22] C.-H. Liu, H. Jiang, and S. Chen, Phys. Rev. B **99**, 125103 (2019).
[23] K. Kawabata, K. Shiozaki, M. Ueda, and M. Sato, Phys. Rev. X **9**, 041015 (2019).
[24] L. Xiao, T. Deng, K. Wang, G. Zhu, Z. Wang, W. Yi, and P. Xue, Nat. Phys. **16**, 761 (2020).
[25] T. Helbig, T. Hofmann, S. Imhof, M. Abdelghany, T. Kiessling, L. W. Molenkamp, C. H. Lee, A. Szameit, M. Greiter, and R. Thomale, Nat. Phys. **16**, 747 (2020).
[26] F. K. Kunst, E. Edvardsson, J. C. Budich, and E. J. Bergholtz, Phys. Rev. Lett. **121**, 026808 (2018).
[27] Z. Yang, K. Zhang, C. Fang, and J. Hu, Phys. Rev. Lett. **125**, 226402 (2020).
[28] Y. Xiong, J. Phys. Commun. **2**, 035043 (2018).
[29] S. Yao and Z. Wang, Phys. Rev. Lett. **121**, 086803 (2018).
[30] F. Song, S. Yao, and Z. Wang, Phys. Rev. Lett. **123**, 170401 (2019).
[31] L. Li, C. H. Lee, S. Mu, and J. Gong, Nat. Commun. **11**, 5491 (2020).
[32] Y. Yi and Z. Yang, Phys. Rev. Lett. **125**, 186802 (2020).
[33] H. Shen, B. Zhen, and L. Fu, Phys. Rev. Lett. **120**, 146402 (2018).
[34] Y.-X. Xiao, K. Ding, R.-Y. Zhang, Z. H. Hang, and C. T. Chan, Phys. Rev. B **102**, 245144 (2020).
[35] W. Tang, X. Jiang, K. Ding, Y.-X. Xiao, Z.-Q. Zhang, C. T. Chan, and G. Ma, Science **370**, 1077 (2020).
[36] K. Wang, A. Dutt, C. C. Wojcik, and S. Fan, Nature (London) **598**, 59 (2021).
[37] K. Wang, A. Dutt, K. Y. Yang, C. C. Wojcik, J. Vučković, and S. Fan, Science **371**, 1240 (2021).
[38] S. Yao, F. Song, and Z. Wang, Phys. Rev. Lett. **121**, 136802 (2018).
[39] H. Wu, L. Jin, and Z. Song, Phys. Rev. B **100**, 155117 (2019).
[40] S. A. Skirlo, L. Lu, and M. Soljačić, Phys. Rev. Lett. **113**, 113904 (2014).
[41] A. Alase and D. L. Feder, Phys. Rev. A **103**, 053305 (2021).
[42] See Supplemental Material at http://link.aps.org/supplemental/10.1103/PhysRevB.105.L081112 for details of non-Hermitian Chern number, the solution of tight-binding model with different boundary conditions, and real-space non-Hermitian Chern number, which includes Ref. [45].
[43] Y. Hatsugai, Phys. Rev. Lett. **71**, 3697 (1993).
[44] T. Fukui, K. Shiozaki, T. Fujiwara, and S. Fujimoto, J. Phys. Soc. Jpn. **81**, 114602 (2012).
[45] F. Song, S. Yao, and Z. Wang, Phys. Rev. Lett. **123**, 246801 (2019).